Proc. Natl. Acad. Sci. USA
Vol. 96, pp. 1732–1737, February 1999
Physiology

Salt restriction induces pseudohypoaldosteronism type 1 in mice expressing low levels of the β-subunit of the amiloride-sensitive epithelial sodium channel

SYLVAIN PRADERVAND*, PIERRE M. BARKER†‡, QING WANG‡§, STEPHEN A. ERNST‡¶, FRIEDRICH BEERMANN‖, BARBARA R. GRUBB†, MICHEL BURNIER§, ANDREA SCHMIDT‖, RENE J. M. BINDELS**, JOHN T. GATZY†, BERNARD C. ROSSIER*††, AND EDITH HUMMLER*††

*Institut de Pharmacologie et de Toxicologie, Université de Lausanne, Rue du Bugnon 27, 1005 Lausanne, Switzerland; †University of North Carolina, School of Medicine, Campus Box 7020, 724 Burnett–Womack Boulevard, Chapel Hill, NC 27599-7020; §Division d'Hypertension, Centre Hospitalier Universitaire Vaudois, Rue P. Decker, 1011 Lausanne, Switzerland; ¶Department of Anatomy and Cell Biology, University of Michigan, Medical Sciences 2, Ann Arbor, MI 488109-0616; ‖Swiss Institute for Experimental Cancer Research, Chemin des Boveresses 155, 1066 Epalinges, Switzerland; and **Department of Cell Physiology, University of Nijmegen, P.O. Box 9101, 6500 HB Nijmegen, The Netherlands

Communicated by Derek A. Denton, University of Melbourne, Parkville, Australia, December 14, 1998 (received for review October 9, 1998)

ABSTRACT **The amiloride-sensitive epithelial sodium channel (ENaC) is a heteromultimer of three homologous subunits (α-, β-, and γ-subunits). To study the role of the β-subunit *in vivo*, we analyzed mice in which the βENaC gene locus was disrupted. These mice showed low levels of βENaC mRNA expression in kidney (≈1%), lung (≈1%), and colon (≈4%). In homozygous mutant βENaC mice, no βENaC protein could be detected with immunofluorescent staining. At birth, there was a small delay in lung-liquid clearance that paralleled diminished amiloride-sensitive Na^+ absorption in tracheal explants. With normal salt intake, these mice showed a normal growth rate. However, *in vivo*, adult βENaC m/m mice exhibited a significantly reduced ENaC activity in colon and elevated plasma aldosterone levels, suggesting hypovolemia and pseudohypoaldosteronism type 1. This phenotype was clinically silent, as βENaC m/m mice showed no weight loss, normal plasma Na^+ and K^+ concentrations, normal blood pressure, and a compensated metabolic acidosis. On low-salt diets, βENaC-mutant mice developed clinical symptoms of an acute pseudohypoaldosteronism type 1 (weight loss, hyperkalemia, and decreased blood pressure), indicating that βENaC is required for Na^+ conservation during salt deprivation.**

Regulation of sodium reabsorption in the kidney is essential for maintaining sodium balance, extracellular-fluid volume, and blood pressure. Principal cells that line the distal part of the renal tubule (in particular, the cortical collecting duct) are targets for aldosterone action, which modulates Na^+ reabsorption. These epithelial cells promote transepithelial Na^+ transport by the amiloride-sensitive epithelial sodium channel (ENaC), located at the apical membrane, facing the lumen, and by the Na^+,K^+-ATPase, located at the basolateral membrane. ENaC constitutes a limiting step in sodium reabsorption (1). The channel is a heterotetrameric protein made of three homologous subunits (α-, β-, and γENaC; refs. 2–4). When expressed in *Xenopus* oocytes, αENaC alone is sufficient to confer a small amiloride-sensitive sodium current (≈50 nA; ref. 5), but β- and γ-subunits are required in addition for maximal channel activity *in vitro* (10–20 μA) (2).

The importance of ENaC in sodium homeostasis has been underlined by the identification of ENaC subunit mutations that result in Liddle's syndrome and the autosomal recessive form of pseudohypoaldosteronism type 1 (PHA-1). When expressed in *Xenopus* oocytes, Liddle mutations enhance the amiloride-sensitive sodium current by increasing the number and open probability of channels at the cell surface (6–9). PHA-1 is a salt-wasting syndrome associated with metabolic acidosis, hyperkalemia, and hyperaldosteronism (10). ENaC mutations causing PHA-1 have been identified in all three ENaC subunits (α-, β-, and γENaC; refs. 11 and 12). In the *Xenopus* oocyte system, Na^+ absorption by mutant ENaC variants is reduced, compared with wild-type ENaC, but not abolished (13).

In vitro, coexpression of β- and γENaC subunits in *Xenopus* oocytes does not confer channel activity at the cell surface, indicating that the αENaC subunit might have a specific and critical role in trafficking the heteromultimeric protein to the plasma membrane (2, 6). Accordingly, inactivation of the αENaC gene locus in mice identified the importance of this subunit in forming functional channels *in vivo* (14). αENaC knockout mice died soon after birth with liquid-filled lungs, underscoring the importance for amiloride-sensitive Na^+ transport to clear lung liquid at birth (14). The inactivation of the γENaC subunit resulted in a severe PHA-1 phenotype and early death (30–36 h after birth) caused by metabolic and electrolyte disturbances (15).

The role of the βENaC subunit *in vivo* is not yet established. Previous studies showed that, for each subunit, both the expression pattern and the regulation in lung, kidney, and colon differ (16–18). ENaC subunits have unique patterns of distribution within different regions of the lung (17). Thus, complete or partial inactivation of the βENaC gene locus may lead to a different phenotype than the one observed for the α- or γENaC knockout mice. When coexpressed in *Xenopus* oocytes, α- and γENaC subunits alone produce an amiloride-sensitive sodium current whose amplitude is 5% of the activity of all three subunits *in vitro* (2). It is not clear whether this reduced level of ENaC activity is sufficient to maintain Na^+ balance *in vivo*.

In the course of generating a mouse model for Liddle's syndrome by the insertion of a stop codon (corresponding to residue R566 in human βENaC) and the selection marker neomycin, we obtained mice with a disruption of the βENaC gene locus. In mice homozygous for the βENaC mutation (βENaC m/m mice), βENaC RNA transcript levels were very low (<4%). βENaC protein was not detectable by immunofluorescence histochemistry in lung and kidney. Under normal conditions, this disruption leads to a mild PHA-1 phenotype and no detectable clinical consequences, but under conditions

Abbreviations: ΔPD_{amil}, amiloride-sensitive potential difference; E*n*, embryonic day *n*; ENaC, amiloride-sensitive epithelial sodium channel; PD, potential difference; PHA-1, pseudohypoaldosteronism type 1.

The publication costs of this article were defrayed in part by page charge payment. This article must therefore be hereby marked "*advertisement*" in accordance with 18 U.S.C. §1734 solely to indicate this fact.

PNAS is available online at www.pnas.org.

‡P.B., Q.W., and S.A.E. contributed equally to this work.
††To whom reprint requests should be addressed. e-mail: bernard.rossier@ipharm.unil.ch and ehummler@pop-server.unil.ch.

of low salt intake, the disruption leads to a severe PHA-1 phenotype.

METHODS

Disruption of the βENaC Gene Locus. Genomic fragments of βENaC were isolated from a 129/Sv mouse genomic library (Stratagene). A 6.8-kb *Hin*dIII fragment encompassing the exon encoding the C terminus was cloned into pBluescript II KS(−) (Stratagene). A mutation (R566Stop) followed by a *Kpn*I restriction site was introduced by site-directed mutagenesis. This plasmid (pBS6.8*Hin*dIIImstop) was used for generating the targeting vector (pHR-BEM). The PGK-neo-poly(A) cassette flanked by two *loxP* sites was inserted in the *Kpn*I site (Fig. 1*A*). A HSV-Tk-poly(A) cassette was inserted towards the 5′ end for negative selection. pHR-BEM was linearized at the unique *Cla*I site and electroporated into HM-1 ES cells (14). Correctly targeted clones were expanded and injected into C57BL/6J blastocysts (19). Male chimeras were bred to C57BL/6J females. Heterozygotes (F_1) were interbred to obtain mice homozygous for the βENaC mutation (F_2 generation).

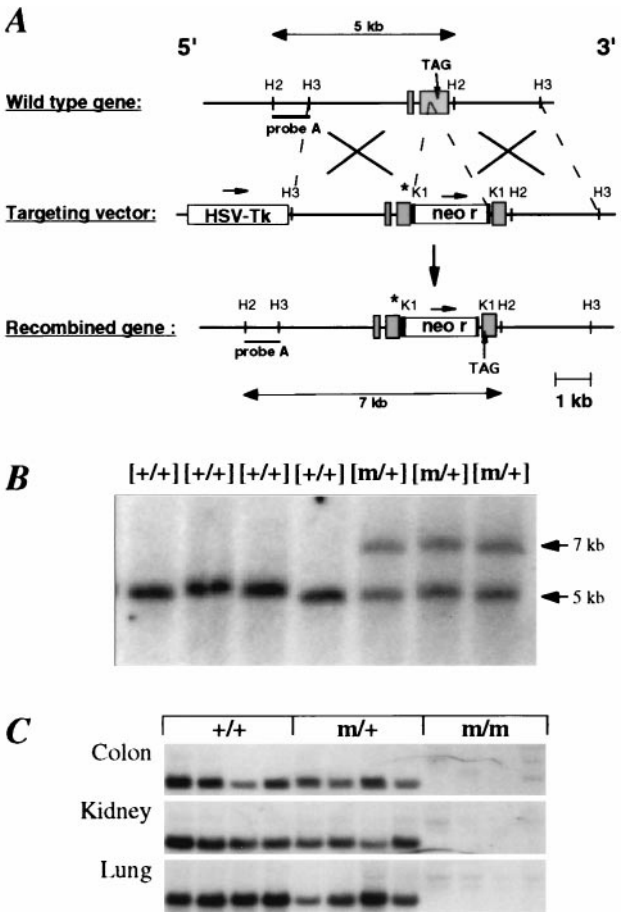

FIG. 1. Gene targeting strategy for the disruption of the mouse βENaC gene locus. (*A*) Structure of the wild-type βENaC gene, the targeting vector, and the predicted targeted locus. The "R566Stop" mutation is indicated (asterisk). Expected fragment sizes of the wild-type and mutated βENaC allele after digestion with *Hin*cII and hybridization with probe A are indicated. H2 = *Hin*cII; H3 = *Hin*dIII; K1 = *Kpn*I. The precise exon–intron structure has not been determined. Identified exons are indicated (shaded box). (*B*) Southern blot analysis of offspring from the breeding of chimeras. Tail DNA was digested with *Hin*cII and hybridized with a 5′ flanking probe (probe A). The βENaC genotype is indicated above each lane. Expected fragment sizes of wild-type (5-kb) and mutant (7-kb) allele are indicated. (*C*) Northern blot analysis of βENaC RNA transcripts from βENaC +/+, m/+, and m/m mice kept on low-salt diets (1 g/kg Na^+). Total RNA (15 μg) from colon, kidney, and lung of each four independent animals was hybridized with βENaC-specific ^{32}P-labeled probes.

Genotyping. Genomic DNA from embryonic stem cell clones and from mouse tails was prepared as described (20). Southern blot analysis was performed on DNA digested with *Hin*cII according to standard procedures by using probe A (Fig. 1*B*). PCR analyses were performed on 100 ng of DNA (32 cycles of 1 min at 94°C, 1 min at 56°C, and 1 min at 72°C). The primers were P_{LS} (5′-CTTCCAAGAGTTCAACTACCG-3′; position is +1,488 to +1,509; 3′ of the translation start site), P_{LAS} (5′-TCTACCAGCTCAGCCACAGTG-3′; position is +1,722 to +1,742; 3′ of the translation start site; indicated primer positions correspond to the rat βENaC cDNA sequence; ref. 2), and P_{neo} (5′-CTGCTATTGGCCGCTGCCCCA-3′; position is +317 to +337; 3′ of the translation start site of the neomycin-resistance gene).

Northern Blot Analysis. Total RNA from colon, kidney, lung, and liver was isolated; 15 μg was run on a 0.8% glyoxal agarose gel and blotted to nylon membranes, according to standard procedures. The membranes were hybridized with random primed ^{32}P-labeled probes for rat α-, β-, and γENaC subunits (2, 5). For quantification of RNA transcripts, loading was normalized by hybridization with a PCR-amplified cDNA probe for mouse glyceraldehyde-3-phosphate dehydrogenase (GAPDH) gene (14). For each group, RNA from four independent animals kept on moderately low-salt diets (1 g/kg Na^+; diet 212; Usine Alimentation Rationelle, Epinay-sur-Orge, France) was analyzed.

Immunocytochemical Analysis and Preparation of Tissues. Kidney and lung from βENaC +/+ and m/m animals were fixed and frozen as described (21). The following two antibodies against βENaC were used: a rabbit antibody against the C terminus of rat βENaC (22) and an affinity-purified guinea pig antibody against the ectodomain of rabbit βENaC (amino acids 244–371). Immunoblots were prepared from a fraction enriched for plasma membranes of *Xenopus* oocytes coexpressing recombinant α-, β-, and γENaC and stained with this antibody, and a single 95-kDa band appeared, corresponding to the size of glycosylated rat βENaC. Immunofluorescent staining was performed on cryostat sections (5 μm) essentially as described (22). The anti-βENaC guinea pig antibody and the rabbit antibody were diluted to 1:300 and 1:500, respectively. The fluorescein isothiocyanate-conjugated secondary antibodies (Jackson ImmunoResearch) were diluted to 1:200. Sections were viewed with a Leitz Aristoplan microscope, and images were recorded on film, digitized, and processed with PHOTOSHOP software, version 3.0 (Adobe Systems, Mountain View, CA).

Lung-Liquid Clearance. To investigate the capacity of the distal lung (terminal bronchioles and alveoli) to absorb liquid, distal-lung explants from embryonic-day-16 (E16) to E18 fetuses were cultured on Transwell collagen-coated membranes in F12/DMEM for 48 h to form liquid-filled multicystic structures. Explants were photographed; 8-(4-chlorophenylthio)-cAMP (10^{-5} M) was added to the culture medium, and explants were rephotographed 24 h later. The change in the number of inflated cysts after the addition of cAMP was used as an index of cAMP-sensitive liquid absorption, which has been shown to be mediated by amiloride-sensitive Na^+ absorption (23). Whole-lung water content of fetal or newborn pups was measured as described (14).

Explant Culture and Bioelectric Measurements. Experiments were performed on tracheal explants from newborn animals and on freshly excised tracheal epithelia from adult animals (14). The activity of the epithelial sodium channel in the distal part of the rectum was measured *in vivo* as the amiloride-sensitive rectal potential difference (ΔPD_{amil}; Q.W., E.H., H. Brunner, B.R., J.-D. Horisberger, and M.B., unpub-

lished work). In mice homozygous for the βENaC mutation and in wild-type mice, ΔPD_{amil} was determined between 4:00 and 6:00 p.m. (the light cycle was from 7:00 a.m. to 7:00 p.m.). Mice were fed normal diets (3 g/kg Na^+; diet A03) or low-salt diets (0.1 g/kg Na^+; diet 212; Ucine Alimentation Rationelle Epinay-sur-Orge) for 5 days before ΔPD_{amil} was measured.

Analytical Procedures and Blood Pressure Measurements. Adult mice (3–5 months old; βENaC +/+, m/+, and m/m) were fed normal diets (3 g/kg Na^+) or low-salt diets (0.1 g/kg Na^+) for 5–10 days before samples were collected. Urinary Na^+ and K^+ excretions were normalized to creatinine concentrations. Blood values were determined from arterial blood taken from the carotid artery after blood pressure was measured. Plasma aldosterone levels were determined by ^{125}I RIA (Coat-A-Count Aldosterone kit, Diagnostic Products, Los Angeles). All assays were run in duplicate. Blood pressure was measured in adult mice (3–5 months old) by carotid catheterization; 4 h after surgery, mean blood pressure from resting mice was recorded over 12 min with a computerized data-acquisition system (24).

Body Weight. βENaC m/m and +/+ mice fed with normal diets (3 g/kg Na^+) were weighed at the same time of day for 6 consecutive days. The body weight (at day 6) was determined as the reference weight. Then, mice were fed the low-salt diet (0.1 g/kg Na^+), and their weights were monitored over 8 more days (days 6–14).

Statistical Analysis. Data are presented as the means ± SEM. Statistical significance was assessed by using unpaired *t* test. $P < 0.05$ was considered the minimum level of significance.

RESULTS

Disruption of the βENaC Gene Locus in Mice. A replacement vector was used to mutate the βENaC gene locus (Fig. 1*A*). Heterozygous mutant embryonic stem cell clones and mice (m/+) were identified by the presence of a 7-kb band (Fig. 1*B*). βENaC m/+ mice were interbred to generate homozygous mutant mice (βENaC m/m). Analysis of a total of 385 mice showed no significant deviation from the expected Mendelian distribution of genotypes (29% βENaC +/+, 46% m/+, and 25% m/m). βENaC m/+ and m/m mice were indistinguishable from +/+ mice in appearance, growth rate, and fertility (data not shown). In βENaC m/+ mice, Northern blot analysis showed reduced expression of the 2.5-kb βENaC mRNA in colon (69 ± 16%; $P = 0.17$), kidney (64 ± 4%; $P < 0.01$), and lung (48 ± 5%; $P < 0.05$; Fig. 1*C*) compared with βENaC +/+ mice. In βENaC m/m mice, low levels of a 4.5-kb RNA transcript were detected in colon (4 ± 2%), kidney (1 ± 1%), and lung (1 ± 1% of wild-type RNA transcript; Fig. 1*C*). In βENaC +/+, m/+, and m/m mice, no significant difference in αENaC mRNA was found in these organs (data not shown). However, in βENaC m/m mice, an up-regulation of the γENaC mRNA was observed in colon (>2× increased; 280 ± 67%; $P < 0.05$) but not in kidney and lung (data not shown).

Immunolocalization of βENaC. An affinity-purified antibody to the ectodomain of the subunit was used to detect expression of both wild-type protein and the mutant βENaC that lacks part of the C terminus. In wild-type mice, both the C-terminal antibody (Fig. 2 *A* and *B*) and the ectodomain antibody (Fig. 2 *C* and *D*) showed localization to late distal tubules and to principal cells of collecting tubules, which comprise most of the collecting tubule epithelium and are known to be the site of ENaC-mediated Na^+ transport. Staining was present throughout the cytoplasm. Specific immunofluorescence staining at the luminal pole, distinct from the cytoplasmic signal, could be resolved only when animals were kept on low-salt diets (data not shown). No specific staining was seen in other nephron segments. In contrast to principal cell immunoreactivity, intercalated cells, which are involved in acid/base balance, were unstained (Fig. 2 *A–D*). In lung of wild-type animals, immunofluorescence staining by the ectodomain antibody was confined to epithelial cells lining the conducting portions of the respiratory tract, including bronchi, bronchioles, and terminal bronchioles (Fig. 2 *G* and *H*). In contrast to the immunolocalization of βENaC in wild-type tissues (Figs. 2 *C* and *G*), no specific staining with the ectodomain antibody was observed in kidney (Fig. 2 *E* and *F*) or lung (Fig. 2 *I* and *J*) of βENaC m/m mice.

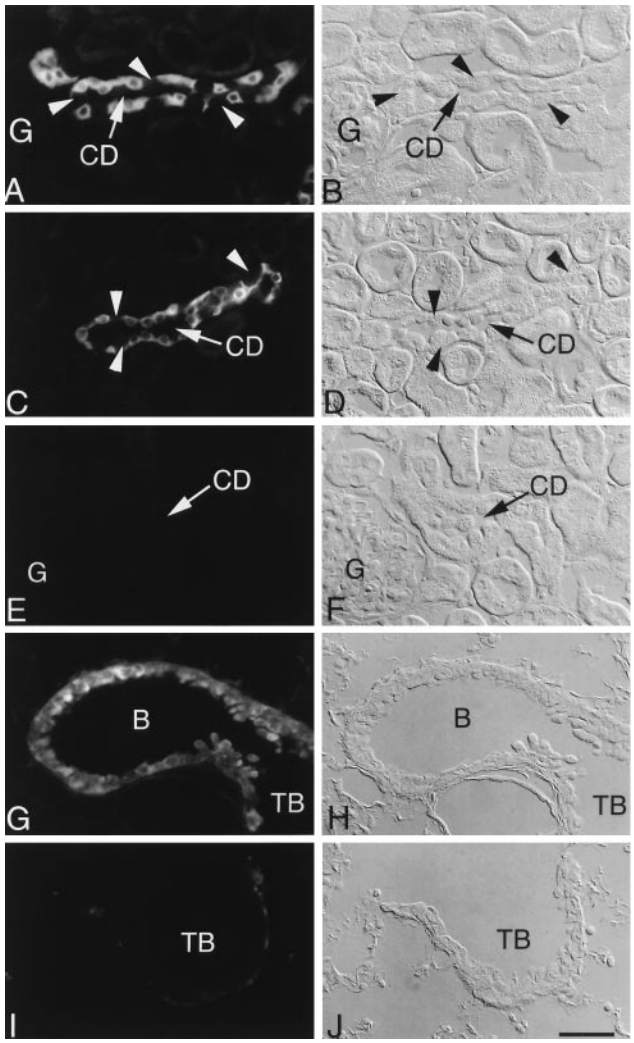

FIG. 2. Immunolocalization of βENaC protein in kidney (*A–F*) and lung (*G–J*) of βENaC +/+ and βENaC m/m mice by using C-terminal antibody (*A* and *B*) and ectodomain antibody (*C–J*). (*Left*) Immunofluorescence. (*Right*) Corresponding Normarski images. In cortical collecting ducts (CD) from wild-type mice (*A–D*), immunofluorescence was present in the cytoplasm of principal cells, whereas intercalated cells (arrowheads) were unreactive. Cells of proximal convoluted tubules and glomeruli (G) were unstained. In contrast, no staining was detected in kidney of βENaC m/m mice (*E* and *F*). In lung of wild-type mice (*G* and *H*), signal was present in bronchioles (B) and terminal bronchioles (TB). No specific immunostaining was present in lung from the βENaC m/m mice (*I* and *J*). The faint, nonspecific fluorescence in *I* is nonepithelial and associated with basement membrane. (Scale bar = 25 μm.)

Role of βENaC in Lung. We assessed perinatal lung-liquid clearance with whole-lung wet/dry weight ratios from E19 fetuses and newborn mice (4, 12, and 24 h after birth; Fig. 3*A*). βENaC m/m mice were able to clear fetal liquid (determined by water content in the lungs) from the air spaces at 12 h of age, when, normally, the lung has cleared most of the residual fetal

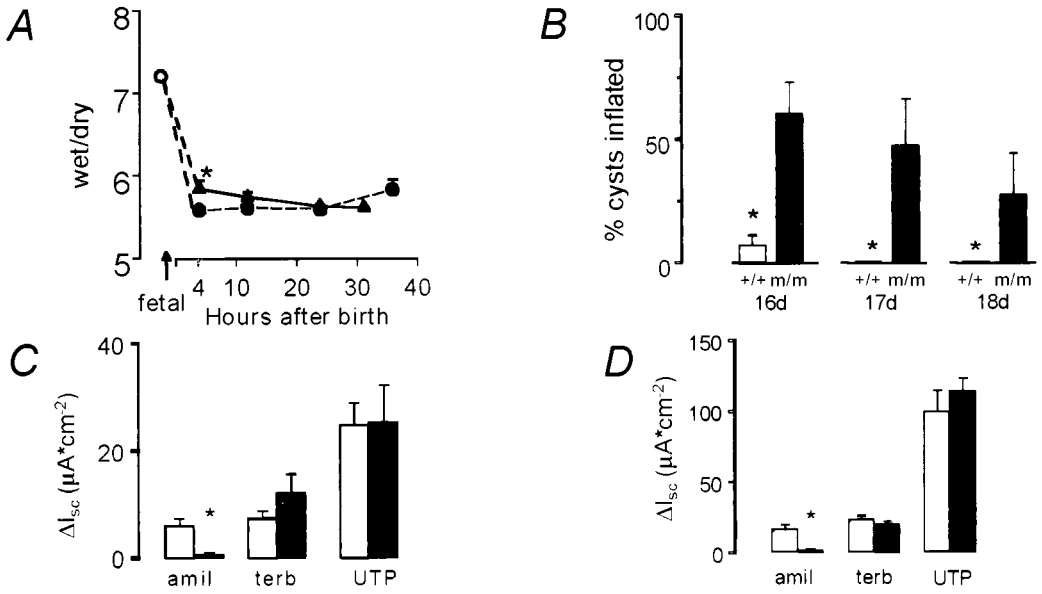

FIG. 3. Liquid absorption in lung explants. (*A*) Mean whole-lung water content (wet/dry weight ratio) in βENaC m/m mice (closed triangles) and βENaC +/+ mice (open circles). *, $P < 0.05$. (*B*) Liquid absorptive capacity measured as percentage of cysts that remained inflated after stimulation by 10^{-5} M cAMP in explants from βENaC m/m (black bars) and +/+ mice (white bars) at E16–E18. (*C* and *D*) Short-circuit currents (ΔI_{sc}) in tracheal explants from newborn (*C*) and adult (*D*) mice. βENaC +/+ (white bars); βENaC m/m (black bars). Treatment with 10^{-4} M amiloride (amil), 3×10^{-4} M terbutaline (terb), and 10^{-4} M UTP, all of which stimulate Cl^- secretion, confirms the viability of the βENaC m/m explants.

liquid. By contrast, at 4 h after birth, lung-liquid clearance was retarded minimally, but significantly, in βENaC m/m mice compared with βENaC wild-type mice (wet/dry ratio; 5.83 ± 0.10 in βENaC m/m mice vs. 5.57 ± 0.05 in βENaC +/+ mice; $n = 52$; $P < 0.05$). In cultured distal-lung explants from E16–E18 fetuses, liquid absorption after exposure to CPT-cAMP in βENaC m/m mice was diminished significantly in comparison with βENaC +/+ explants ($P < 0.01$; Fig. 3*B*). Amiloride-sensitive short-circuit current in freshly excised newborn (Fig. 3*C*) and adult (Fig. 3*D*) trachea was diminished significantly in βENaC m/m compared with wild-type mice. Amiloride-sensitive Na^+ transport in explants from neonate βENaC m/+ mice was not significantly different from wild-type explants (data not shown). Despite a 6-fold reduction in ENaC-mediated transport in trachea, neonate βENaC m/m mice were still able to clear their lungs of liquid. This result is consistent with findings in γENaC knockout (15) and αENaC transgenic knockout mice (25), indicating that relatively low amiloride-sensitive Na^+ conductance clears lungs of liquid at birth and keeps them dry after birth.

Role of βENaC in Kidney and Colon: Normal-Salt Diet. In colon, βENaC m/m mice exhibited a significant 3-fold lower ENaC-mediated transport measured by ΔPD_{amil} than βENaC +/+ mice (Fig. 4*A*; $P < 0.01$). In response to normal-salt diets (3 g/kg Na^+), βENaC m/m mice excreted significantly more Na^+ and K^+ in urine than wild-type mice (Fig. 4*B*; for each group, $n = 17$; $P < 0.05$), but the $[Na^+]/[K^+]$ ratio did not differ significantly ($[Na^+]/[K^+]$ ratios were 1.13 ± 0.14 for βENaC m/m vs. 0.96 ± 0.11 for βENaC +/+). This result might be explained by an enhanced food intake, thus compensating for salt wasting. βENaC m/m mice exhibited normal values of serum $[Na^+]$ [151.7 ± 1.0 mM in βENaC m/m ($n = 8$) vs. 148.7 ± 0.8 mM in βENaC +/+ mice ($n = 7$)], of serum $[K^+]$ [4.49 ± 0.24 mM in βENaC m/m ($n = 8$) vs. 4.29 ± 0.09 mM in βENaC +/+ mice ($n = 7$)], and of blood pH (Fig. 4*C*). However, a significant decrease in $[HCO_3^-]$ (Fig. 4*C*) and lower PCO_2 [32.0 ± 1.5 mmHg in βENaC m/m ($n = 7$) vs. 39.6 ± 1.1 mmHg in βENaC +/+ ($n = 5$); 1 mmHg = 133 Pa; $P < 0.01$] indicate a compensated metabolic acidosis. Furthermore, we observed a significant 1.8-fold higher plasma aldosterone level in βENaC m/m mice (Fig. 4*D*). Thus, with normal-salt diets, βENaC m/m mice exhibit a compensated PHA-1 phenotype.

Low-Salt Diet. During feeding with low-salt diets (0.1 g/kg Na^+), βENaC m/m mice continuously lost body weight. Significant differences between βENaC m/m and +/+ mice were

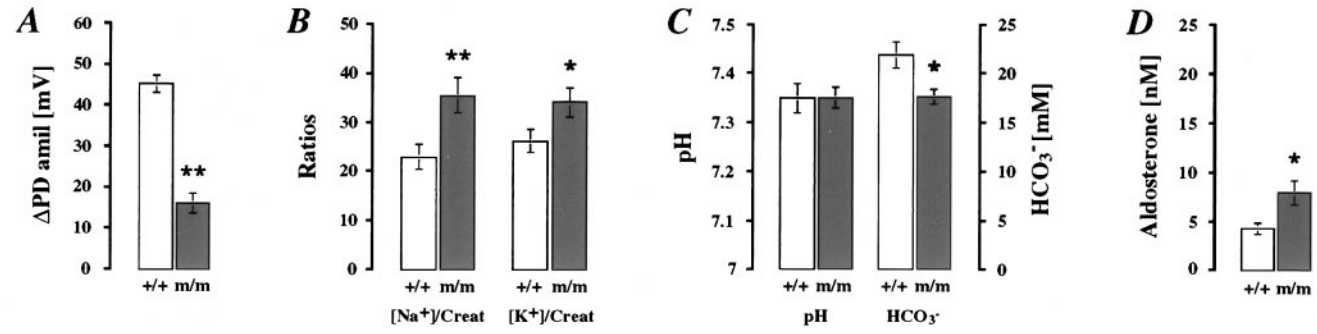

FIG. 4. Physiological measurement in adult βENaC +/+ (white bars) and m/m (dark bars) mice on normal-salt (3 g/kg Na^+) diets. (*A*) *In vivo* measurements of ΔPD_{amil} (βENaC +/+, $n = 16$; βENaC m/m, $n = 17$). **, $P < 0.01$. (*B*) Relative values of urinary Na^+ and K^+ normalized with creatinine (Creat; for each group, $n = 17$). *, $P < 0.05$; **, $P < 0.01$. (*C*) Arterial blood pH and HCO_3^- (βENaC +/+, $n = 5$; βENaC m/m, $n = 7$). *, $P < 0.05$. (*D*) Plasma aldosterone concentrations (nM; for each group, $n = 7$). *, $P < 0.05$.

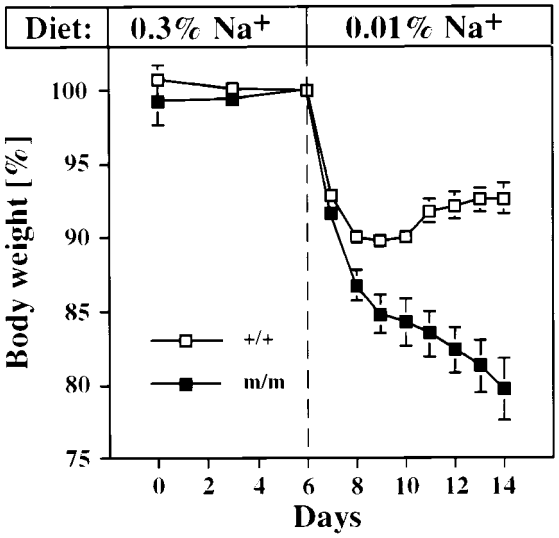

FIG. 5. Body-weight measurements in βENaC +/+ ($n = 12$; open squares) and m/m ($n = 8$; closed squares) mice. Animals were kept 6 days (days 0–6) on normal-salt diets (3 g/kg Na^+), which then were replaced by low-salt diets (0.1 g/kg Na^+) for 8 more days (days 6–14). Body weights of each group are indicated as percentage of reference weight (100% at day 6). Mice were weighed daily at the same time.

evident by the second day of treatment (Fig. 5; $P < 0.01$). After 8 days of the low-salt diet (day 14; Fig. 5), βENaC m/m mice had lost ≈20% (20.3 ± 5.9%) of their initial weight, whereas the controls had lost only ≈7% (6.3 ± 3.6%; $P < 0.01$). In blood plasma, [K^+] was elevated (Fig. 6*A*; $P < 0.01$), whereas [Na^+] was in the normal range [m/m 152.1 ± 1.5 mM in βENaC m/m mice ($n = 7$) vs. 151.5 ± 2.1 mM in βENaC +/+ mice ($n = 7$)]. In urine, excretion of Na^+ and K^+ did not differ significantly between both groups fed with low-salt diets, even though [Na^+]/[creatinine] in βENaC m/m mice was increased 3-fold compared with the controls (Fig. 6*B*). Aldosterone was stimulated in both groups on low-salt diets (2.6× in βENaC m/m mice and 2.8× in βENaC +/+ mice; see Fig. 4*C*) but was increased 1.6× in βENaC m/m mice compared with their controls (Fig. 6*C*; $P < 0.01$). *In vivo* measurements of ΔPD_{amil} in distal colon showed that βENaC m/m mice, when kept on low-salt diets, are able to increase their sodium transport (Fig. 4*A*), but ENaC activity is reduced in comparison with βENaC +/+ mice (Fig. 6*D*; $P < 0.01$). The consequences of low-salt diet (0.1 g/kg Na^+) on mean blood pressure were also determined (Fig. 6*E*). In βENaC m/m mice on low-salt diets, mean blood pressure was reduced in comparison to m/m mice kept on normal-salt diets ($P < 0.05$; Fig. 6*E*). In controls, mean blood pressure did not change with low-salt diets, indicating that normal βENaC expression is required for Na^+ conservation during salt deprivation.

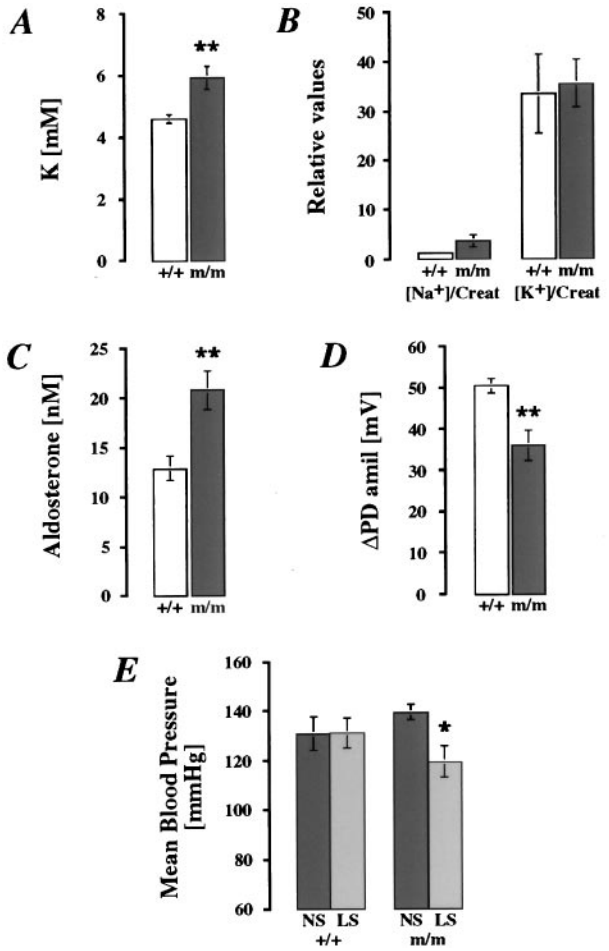

FIG. 6. Physiologic measurements in adult βENaC m/m (black bars) and +/+ (white bars) mice on low-salt diets (0.1 g/kg Na^+; *A–D*). (*A*) Plasma K^+. For each group, $n = 7$. **, $P < 0.01$. (*B*) Relative values of urinary Na^+ and K^+ normalized with creatinine (Creat). For βENaC +/+, $n = 7$; for βENaC m/m, $n = 6$. (*C*) Plasma aldosterone levels (nM). For each group, $n = 6$. **, $P < 0.01$. (*D*) *In vivo* measurements of ΔPD_{amil}. For βENaC +/+, $n = 6$; for βENaC m/m, $n = 7$. **, $P < 0.01$. (*E*) Mean blood-pressure measurements in βENaC +/+ ($n = 7$) and m/m ($n = 8$) mice on normal-salt diets (NS; 3 g/kg Na^+) and low-salt diets (LS; 0.1 g/kg Na^+). *, $P < 0.05$.

DISCUSSION

Disruption of the βENaC Gene Locus. Our strategy resulted in (*i*) large decreases of βENaC RNA transcripts in kidney, colon, and lung, (*ii*) the absence of βENaC protein expression, and (*iii*) reduced ENaC activity as indicated by several physiological parameters. These findings were unexpected, because the insertion of a stop codon, which is analogous to the mutation found in patients with Liddle's syndrome, should not affect RNA levels and instead lead to increased ENaC density and activity (6, 9, 26). We suggest that the insertion of an additional selection marker [in this study, the insertion of the neomycin-resistance gene (*neo*) into 3′ untranslated sequences] resulted in destabilization and/or degradation of the βENaC mRNA transcripts (27). *In vivo,* the presence of *neo* could interfere with the expression of the corresponding gene locus or down-regulate gene activity (28). For example, inclusion of a neo cassette in an intron interfered with the expression of the *Gbx2* gene (29), presumably because the neo cassette contained cryptic splice sites (30). Preliminary data indeed indicated that removing the neo cassette by using the Cre-loxP-mediated recombination system (Cre-expressing mice) efficiently restored βENaC expression in βENaC m/m mice (S.P., Q.W., S.E., M.B., F.B., E.H., and B.R., unpublished data).

Role of βENaC *in Vivo*. Reduced ENaC activity is still present in colon and lung of βENaC m/m mice. In contrast to αENaC knockout mice, in which the inactivation of α-subunit causes a fatal inability to clear lung-liquid, βENaC m/m mice showed only a minor delay in lung-liquid clearance in the first hours of life (ref. 15; Fig. 3 *A–D*). Similarly, animals in which the γENaC subunit was inactivated could still clear lung liquid at birth. However, they died soon after birth with PHA-1 symptoms like urinary salt wasting and hyperkalemia (15). In βENaC m/m mice, the absorptive capacity could be provided by channels associated with only α- or γENaC subunits or those in combination with residual βENaC subunits. Therefore, ENaC function might be sufficient in the near absence of

βENaC expression to maintain salt and water homeostasis under normal dietary conditions. Fully active ENaCs, however, are required to maintain total body water and electrolyte balance under low-salt dietary conditions. Therefore, βENaC m/m mice present a model for studying the role of the βENaC subunit *in vivo*.

Salt Restriction Induces PHA-1 in βENaC m/m Mice. The βENaC m/m and the previously described αENaC knockout transgenic mice present two different types of PHA-1 mouse models. In αENaC knockout transgenic mice, the transgene is no longer under aldosterone control and constitutes the limiting subunit for ENaC activity (25). In βENaC m/m mice, increased plasma aldosterone concentrations can still act on βENaC as well as on αENaC and/or γENAC subunit expression. Indeed, in these animals, an up-regulation of γENaC mRNA in colon has been observed. On normal-salt diets, βENaC m/m mice can maintain plasma $[Na^+]$, $[K^+]$, and blood pressure in the normal range. However, on low-salt diets, βENaC m/m mice cannot sufficiently adapt to maintain sodium balance, and they show clinical symptoms of an acute PHA-1, although Na^+ transport was increased in colon. In humans, PHA-1 is a heterogeneous clinical syndrome ranging from severe salt loss in infancy to a clinically less severe syndrome aggravated by salt depletion (11, 31–33). With respect to these clinical cases described, the βENaC m/m mice present a mouse model which is appropriate to the human situation.

In the present study, βENaC subunit limits channel function under conditions like low-salt intake. βENaC m/m mice try to respond to this "challenge" by stimulating the renal–adrenal axis (elevated plasma aldosterone levels). In these mice, mutation of the mouse βENaC gene locus could confer salt resistance. This assumption is of particular interest, because, in human populations, PHA-1 mutations might be silent; a PHA-1 phenotype is provoked only by environmental challenge. Our study emphasizes the importance of all three subunits in forming functional and aldosterone-regulated channels in kidney and colon under different dietary Na^+ conditions.

We thank Jean-Daniel Horisberger and Olivier Bonny for suggestions on the manuscript, H.-P. Gäggeler for help with photographic work, L. and Y. Guibert for taking care of the animals, and H. Yao for help in conducting the immunofluorescence studies. S.A.E. was financed by National Institutes of Health Grant DK34933, and R.J.M.B. was financed by Dutch Kidney Foundation Grant C94.1348. This work was supported by Swiss National Science Foundation Grants 32-52471.97 to M.B., 31-43384.95 to B.C.R. and 31-52943.97 to E.H. and a grant from the Cystic Fibrosis Foundation.

1. Rossier, B. C. & Palmer, L. G. (1992) in *The Kidney: Physiology and Pathophysiology,* eds. Seldin, D. W. & Giebisch, G. (Raven, New York), pp. 1373–1409.
2. Canessa, C. M., Schild, L., Buell, G., Thorens, B., Gautschi, I., Horisberger, J. D. & Rossier, B. C. (1994) *Nature (London)* **367,** 463–467.
3. Firsov, D., Gautschi, I., Merillat, A.-M., Rossier, B. C. & Schild, L. (1998) *EMBO J.* **17,** 344–352.
4. Kosari, F., Sheng, S., Li, J., Mak, D.-O. D., Foskett, K. & Kleyman, T. R. (1998) *J. Biol. Chem.* **273,** 13469–13474.
5. Canessa, C. M., Horisberger, J. D. & Rossier, B. C. (1993) *Nature (London)* **361,** 467–470.
6. Firsov, D., Schild, L., Gautschi, I., Mérillat, A.-M., Schneeberger, E. & Rossier, B. C. (1996) *Proc. Natl. Acad. Sci. USA* **93,** 15370–15375.
7. Snyder, P. M., Price, M. P., McDonald, F. J., Adams, C. M., Volk, K. A., Zeiher, B. G., Stokes, J. B. & Welsh, M. J. (1995) *Cell* **83,** 969–978.
8. Schild, L., Lu, Y., Gautschi, I., Schneeberger, E., Lifton, R. P. & Rossier, B. C. (1996) *EMBO J.* **15,** 2381–2387.
9. Shimkets, R. A., Warnock, D. G., Bositis, C. M., Nelson-Williams, C., Hansson, J. H., Schambelan, M., Gill, J. R., Jr., Ulick, S., Milora, R. V., Findling, J. W., *et al*. (1994) *Cell* **79,** 407–414.
10. Cheek, D. B. & Perry, J. W. (1957) *Arch. Dis. Child.* **33,** 252–256.
11. Chang, S. S., Gründer, S., Hanukoglu, A., Rösler, A., Mathew, P. M., Hanukoglu, I., Schild, L., Lu, Y., Shimkets, R. A., Nelson-Williams, C., *et al*. (1996) *Nat. Genet.* **12,** 248–253.
12. Strautnieks, S. S., Thompson, R. J., Gardiner, R. M. & Chung, E. (1996) *Nat. Genet.* **13,** 248–250.
13. Hummler, E. (1998) *Exp. Nephrol.* **6,** 265–271.
14. Hummler, E., Barker, P., Gatzy, J., Beermann, F., Verdumo, C., Schmidt, A., Boucher, R. & Rossier, B. C. (1996) *Nat. Genet.* **12,** 325–328.
15. Barker, P. M., Ngugen, M. S., Gatzy, J. T., Grubb, B., Norman, H., Hummler, E., Rossier, B., Boucher, R. C. & Koller, B. (1998) *J. Clin. Invest.* **102,** 1634–1640.
16. Renard, S., Voilley, N., Bassilana, F., Lazdunski, M. & Barbry, P. (1995) *Eur. J. Physiol.* **430,** 299–307.
17. Farman, N., Talbot, C. R., Boucher, R., Fay, M., Canessa, C., Rossier, B. & Bonvalet, J. P. (1997) *Am. J. Physiol.* **272,** C131–C141.
18. Matsushita, K., McCray, P. B., Sigmund, R. D., Welsh, M. J. & Stokes, J. B. (1996) *Am. J. Physiol.* **271,** L332–L339.
19. Hummler, E., Cole, T. J., Blendy, J. A., Ganss, R., Aguzzi, A., Schmid, W., Beermann, F. & Schütz, G. (1994) *Proc. Natl. Acad. Sci. USA* **91,** 5647–5651.
20. Schmidt, A., Tief, K., Foletti, A., Hunziker, A., Penna, D., Hummler, E. & Beermann, F. (1998) *Brain Res. Brain Res. Protoc.* **3,** 54–60.
21. Staub, O., Yeager, H., Plant, P. J., Kim, H., Ernst, S. A. & Rotin, D. (1997) *Am. J. Physiol.* **272,** C1871–C1880.
22. Duc, C., Farman, N., Canessa, C. M. & Bonvalet, J.-P. (1994) *J. Cell Biol.* **127,** 1907–1921.
23. Olver, R. E., Ramsden, C. A., Strang, L. B. & Walters, D. V. (1986) *J. Physiol.* **376,** 321–340.
24. Wiesel, P., Mazzolai, L., Nussberger, J. & Pedrazzini, T. (1997) *Hypertension* **29,** 1025–1030.
25. Hummler, E., Barker, P., Talbot, C., Wang, Q., Verdumo, C., Grubb, B., Gatzy, J., Burnier, M., Horisberger, J.-D., Beermann, F., *et al*. (1997) *Proc. Natl. Acad. Sci. USA* **94,** 11710–11715.
26. Schild, L., Canessa, C. M., Shimkets, R. A., Warnock, D. G., Lifton, R. P. & Rossier, B. C. (1995) *Proc. Natl. Acad. Sci. USA* **92,** 5699–5703.
27. Shaw, G. & Kamen, R. (1986) *Cell* **46,** 659–667.
28. Nagy, A., Moens, C., Ivanyi, E., Pawling, J., Gertsenstein, M., Hadjantonakis, A.-K., Pirity, M. & Rossant, J. (1998) *Curr. Biol.* **8,** 661–664.
29. Wassarman, K. M., Lewandoski, M., Campbell, K., Joyner, A. L., Rubenstein, J. L. R., Martinez, S. & Martin, G. R. (1997) *Development (Cambridge, U.K.)* **124,** 2923–2934.
30. Meyers, E. N., Lewandoski, M. & Martin, G. R. (1998) *Nat. Genet.* **18,** 136–141.
31. Kuhnle, U., Hinkel, G. K., Huble, W. & Reichelt, T. (1996) *Horm. Res.* **46,** 124–129.
32. Rösler, A. (1984) *J. Clin. Endocrinol. Metab.* **59,** 689–700.
33. Kuhnle, U. (1997) *Mol. Cell. Endocrinol.* **133,** 77–80.